LEARNING APPROACH TO THE ACTIVE COMPLIANCE CONTROL OF MULTI-ARM ROBOTS COUPLED THROUGH A FLEXIBLE OBJECT

Christian von Albrichsfeld, Mikhail Svinin*, and Henning Tolle
Darmstadt University of Technology, Institute of Control Engineering
Department of Control Systems Theory & Robotics
Landgraf-Georg-Strasse 4, D-64283 Darmstadt
E-Mail: alb@rt.e-technik.th-darmstadt.de

Keywords: Learning control; compliance control; multi-arm robots.

Abstract

This paper presents a quasi-static model and a control strategy for N robot arms cooperating through a concerning its compliant behaviour partly unknown flexible object. The control strategy is based on the position/force decomposition of an extended $6N$-dimensional space. The strategy includes feedforward and feedback levels. The feedback level is organized in the form of an active compliance control law. An AMS-based learning approach is used to accommodate the compliance behaviour of the system and utilized as an additional feedforward loop in the control system. The applicability of the control strategy is verified by simulation.

1 Introduction

The importance of multi-arm robotic systems has been realized by the robotics community in many applications where the object to be manipulated may be too heavy, too large, or too flexible. In literature a number of control methods for coordinated multiple robot arms have been developed. These strategies are based on pure position control schemes [1], master/slave control schemes [2] hybrid position/force control approaches [3, 4], active stiffness/compliance control schemes [5], or model-based dynamic control schemes [6, 7]. In spite of the significance of the results obtained in the field of multi-arm robots, it should be pointed out that practically all of them have been formulated for the case of rigid body handling. In addition most of the control methods need a detailed knowledge of the complex static and dynamic model of the robots and the object for achieving good results.

In this paper we will deal with the task of controlling the motion and internal force of a flexible object. The control system must take into account the elastic properties of the object. To this purpose we formulate a control strategy including an active compliance control law on the Cartesian level. To accommodate to the unknown compliance of the system, an AMS-based learning control loop is proposed. By exploitation of the properties of the closed kinematic chain the complex nonlinear compliance is learned during the repetitive execution of a task and used in an additional feedforward loop for controlling the robots. The learning procedure is based on the concept of a virtual object.

This paper is organized as follows. First, in Section 2, basic assumptions and notations are introduced, and the quasi-static model of the system under consideration is developed. Section 3 summarizes the inter-arm coordination strategy which is completely formulated in task-oriented coordinates. Next, the learning control loop and simulation results are presented in Sections 4 and 5. Finally, Section 6 presents conclusions.

2 Mathematical Model of the System

A sketch of the system under consideration is depicted in Figure 1 where the following coordinate frames are introduced: $\mathcal{W}$ is an inertial reference frame; $\mathcal{L}$ is a frame which is rigidly tied with the object and is placed at its center of inertia; $\mathcal{H}_i$ is a frame associated with the end-effector of i-th manipulator; $\mathcal{G}_i$ is a frame which is rigidly tied with the object and is placed at the i-th point of grasping of the object, $i = \overline{1, N}$.

The structural properties of the elastic object can be described by using the so-called assumed modes method [8]. The vectors of small translational $\mathbf{u}(\boldsymbol{\rho})$ and angular $\boldsymbol{\theta}(\boldsymbol{\rho})$ elastic displacements, considered at the point $\boldsymbol{\rho}$ with respect to the reference frame $\mathcal{L}$, are represented in the following form:

$$\mathbf{u}(\boldsymbol{\rho}) = \sum_{j=1}^{m} \boldsymbol{\varphi}_j(\boldsymbol{\rho})\, \eta_j, \qquad \boldsymbol{\theta}(\boldsymbol{\rho}) = \sum_{j=1}^{m} \boldsymbol{\psi}_j(\boldsymbol{\rho})\, \eta_j, \qquad (1)$$

*On leave from Automation & Technical Physics Department, Irkutsk Scientific Center, Russian Academy of Science, Lermontov Str. 281, Irkutsk 664033, Russia.

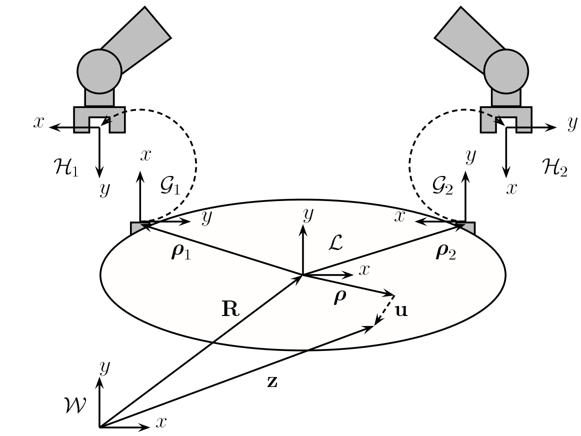

Figure 1: Multi-arm system with a flexible object.

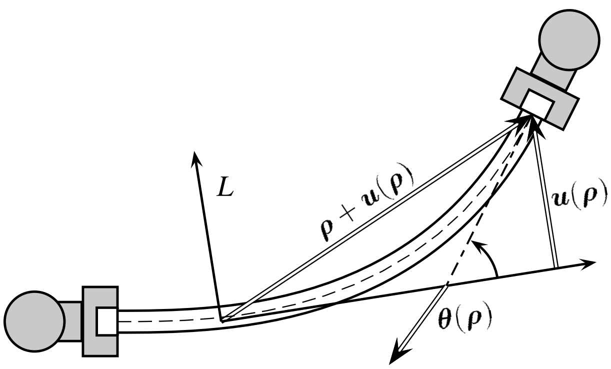

Figure 2: Elastic displacements of the object.

where $\boldsymbol{\varphi}_j(\boldsymbol{\rho})$, $\boldsymbol{\psi}_j(\boldsymbol{\rho})$ are space dependent shape vector functions, and η_j are the modal coordinates of the object.

The static equations of the deformable object grasped by the manipulators can be found in [9]. To formulate the control strategy we introduce the simplified static model of a virtual object, where the distributed compliance is concentrated at the grasping points $\boldsymbol{\rho}_i$. The translational and angular elastic displacements $\mathbf{u}(\boldsymbol{\rho}_i)$ and $\boldsymbol{\theta}(\boldsymbol{\rho}_i)$ of each spring are represented as generalized 6-dimensional springs with the combined extension $\boldsymbol{X}_{c_i} = \{\mathbf{u}(\boldsymbol{\rho}_i)^{\mathrm{T}}, \boldsymbol{\theta}(\boldsymbol{\rho}_i)^{\mathrm{T}}\}^{\mathrm{T}}$ at each grip frame connecting the object with the manipulator (see Figure 5). As can be derived from the above mentioned equations the static displacements of the introduced springs are solely a function of the forces applied by the cooperating robots.

3 Coordination Strategy

Here in this section, an inter-arm coordination strategy is presented, which has been introduced in a modified version in [5]. The strategy contains three basic elements: a planning module, a feed-forward and a feed-back position/force coordination (see Figure 3).

The planning module provides the nominal payload motion $\boldsymbol{X}_{L,n}(t) \in \Re^6$, the desired internal forces

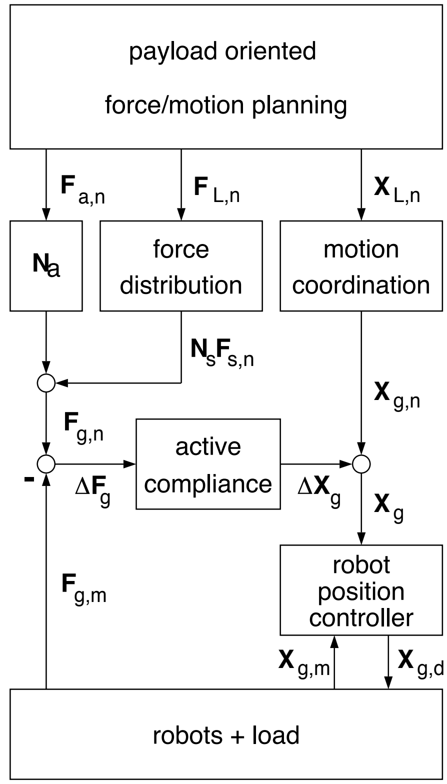

Figure 3: Coordination strategie.

$\boldsymbol{F}_{a,n}(t) \in \Re^{6(N-1)}$, and by use of the dynamic model of the object, the nominal synergistic forces to be applied to the object $\boldsymbol{F}_{L,n}(t) = \boldsymbol{F}_{ext,n}(t) + \boldsymbol{F}_{acc,n}(t) + \boldsymbol{F}_{grav,n}(t) \in \Re^6$, taking into account external forces to be excerted to the environment, acceleration and gravitational forces as a function of time t.

The feed-forward coordinator is divided into two parts: the motion coordinator and the force/torque coordinator. The motion coordinator derives a combined nominal motion trajectory $\boldsymbol{X}_{g,n}(t)$, where $\boldsymbol{X}_g = \left\{\boldsymbol{X}_{g_1}^{\mathrm{T}}, \boldsymbol{X}_{g_2}^{\mathrm{T}}, \ldots, \boldsymbol{X}_{g_N}^{\mathrm{T}}\right\}^{\mathrm{T}} \in \Re^{6N}$ represents the generalized coordinates of the grip frames, by a "rigid" transformation from the reference frame to the grapple frames corresponding to the vectors $\boldsymbol{\rho}_i$ (i = 1..N). Feedforward force/torque coordination is achieved by a linear force distribution law $\boldsymbol{F}_{g,n} = \{\boldsymbol{J}_q^{\mathrm{T}}\}^{\#}\boldsymbol{F}_{L,n} + \boldsymbol{N}_a\boldsymbol{F}_{a,n}$, where $\boldsymbol{F}_g = \left\{\boldsymbol{F}_{g_1}^{\mathrm{T}}, \boldsymbol{F}_{g_2}^{\mathrm{T}}, \ldots, \boldsymbol{F}_{g_N}^{\mathrm{T}}\right\}^{\mathrm{T}} \in \Re^{6N}$ is the combined vector of forces and torques applied to the object from the manipulators. Synergistic forces/torques are distributed by the matrix $\{\boldsymbol{J}_q^{\mathrm{T}}\}^{\#}$, the {1,2,3}-generalized inverse (see [10]) of the $\{\boldsymbol{J}_q^{\mathrm{T}}\}$ matrix, satisfying the condition $\{\boldsymbol{J}_q^{\mathrm{T}}\}\{\boldsymbol{J}_q^{\mathrm{T}}\}^{\#} = \boldsymbol{I}$. In this equation $\boldsymbol{J}_q = \{\boldsymbol{J}_{q_1}^{\mathrm{T}} \vdots \boldsymbol{J}_{q_2}^{\mathrm{T}} \vdots \ldots \vdots \boldsymbol{J}_{q_N}^{\mathrm{T}}\}^{\mathrm{T}} \in \Re^{6N\times 6}$ is the rigid Jacobian of the object. It is made up of the Jacobians of each gripping frame represented in the form:

$$\boldsymbol{J}_{q_i} = \begin{bmatrix} \boldsymbol{I} & \Omega^{\mathrm{T}}(\boldsymbol{\rho}_i) \\ \boldsymbol{O} & \boldsymbol{I} \end{bmatrix}, \qquad (2)$$

where $\boldsymbol{O} \in \Re^{3\times 3}$ is the null matrix and $\boldsymbol{\Omega}(\cdot) \in \Re^{3\times 3}$ is the skew-symmetric operator such that $\boldsymbol{\Omega}(\boldsymbol{a}) \cdot \boldsymbol{b} \equiv \boldsymbol{a} \times \boldsymbol{b}$. The planned anergistic forces $\boldsymbol{F}_{a,n}$ are distributed to the cooperating arms by use of the matrix $\boldsymbol{N}_a$ which is introduced in the next paragraph.

The feedback coordinator, constructed in the form of an active compliance law, derives corrections of the nominal motion trajectory $\Delta \boldsymbol{X}_g$ based on the tracking errors of the nominal force trajectory $\Delta \boldsymbol{F}_g$. To formulate the active compliance law, we decompose the vectors $\dot{\boldsymbol{X}}_g$ and $\boldsymbol{F}_g = \boldsymbol{F}_{g,n}$ which are the Cartesian level inputs to the manipulators' control system. The decomposition is based upon two partitioning schemes. The first scheme is given by the force distribution law. The columns of $\{\boldsymbol{J}_q^{\mathrm{T}}\}^{\#}$ matrix span the space of synergistic forces $\mathcal{S}_s = \mathcal{R}(\{\boldsymbol{J}_q^{\mathrm{T}}\}^{\#})$, and the null space of $\boldsymbol{J}_q^{\#}$ is referred to as the space of anergistic forces $\mathcal{S}_a = \mathcal{N}(\boldsymbol{J}_q^{\#})$. The second partitioning scheme is based upon the matrix $\boldsymbol{J}_q$. It defines the space of rigid body motion $\mathcal{S}_r = \mathcal{R}(\boldsymbol{J}_q)$ and the space of elastic deformations $\mathcal{S}_e = \mathcal{N}(\{\boldsymbol{J}_q^{\mathrm{T}}\})$.

Calculating the orthonormal bases of the spaces introduced, we can represent arbitrary displacement and force vectors $\dot{\boldsymbol{X}}_g$ and $\boldsymbol{F}_g$ as follows

$$\dot{\boldsymbol{X}}_g = [\boldsymbol{N}_r \boldsymbol{N}_e] \cdot \begin{bmatrix} \dot{\boldsymbol{X}}_r \\ \dot{\boldsymbol{X}}_e \end{bmatrix} \quad \boldsymbol{F}_g = [\boldsymbol{N}_s \boldsymbol{N}_a] \cdot \begin{bmatrix} \boldsymbol{F}_s \\ \boldsymbol{F}_a \end{bmatrix}, \quad (3)$$

where: $\boldsymbol{N}_r \in \Re^{6N \times 6}$, $\boldsymbol{N}_s \in \Re^{6N \times 6}$, $\boldsymbol{N}_e \in \Re^{6N \times 6(N-1)}$, and $\boldsymbol{N}_a \in \Re^{6N \times 6(N-1)}$ are base matrices of the spaces $\mathcal{S}_r, \mathcal{S}_s, \mathcal{S}_e, \mathcal{S}_a$; $\dot{\boldsymbol{X}}_e, \boldsymbol{F}_a, \dot{\boldsymbol{X}}_r$ and $\boldsymbol{F}_s$ are corresponding components of $\dot{\boldsymbol{X}}_g$ and $\boldsymbol{F}_g$ in these spaces. Using the orthogonal properties of the above-introduced spaces, we can derive the inversion of (3) by multiplying with $[\boldsymbol{N}_r \boldsymbol{N}_e]^{\mathrm{T}}$, $[\boldsymbol{N}_s \boldsymbol{N}_a]^{\mathrm{T}}$ respectively.

$$\begin{bmatrix} \dot{\boldsymbol{X}}_r \\ \dot{\boldsymbol{X}}_e \end{bmatrix} = \begin{bmatrix} \boldsymbol{N}_r^{\mathrm{T}} \\ \boldsymbol{N}_e^{\mathrm{T}} \end{bmatrix} \cdot \dot{\boldsymbol{X}}_g, \quad \begin{bmatrix} \boldsymbol{F}_s \\ \boldsymbol{F}_a \end{bmatrix} = \begin{bmatrix} \boldsymbol{N}_s^{\mathrm{T}} \\ \boldsymbol{N}_a^{\mathrm{T}} \end{bmatrix} \cdot \boldsymbol{F}_g. \quad (4)$$

For motion-servoed manipulators the active compliance law contains a mixture of the following generalized spring and generalized damper terms

$$\Delta \boldsymbol{X}_g = \alpha_p \boldsymbol{C}_{tot} \Delta \boldsymbol{F}_g, \quad \Delta \dot{\boldsymbol{X}}_g = \alpha_v \boldsymbol{C}_{tot} \Delta \boldsymbol{F}_g, \quad (5)$$

with $\Delta \boldsymbol{F}_g$ denoting the difference between nominal and measured concatenated force/torque vectors, $\Delta \boldsymbol{X}_g$ and $\Delta \dot{\boldsymbol{X}}_g$ the position and velocity corrections to be applied to the nominal motion commands, α_p and α_v the scalar gains to be adjusted.

To derive the total compliance matrix $\boldsymbol{C}_{tot}$, at first we define the end-point compliance of the object with fixed rigid coordinates. It is defined by the blockdiagonal matrix $\boldsymbol{C}_o = diag\{\boldsymbol{C}_1, \boldsymbol{C}_2, ...\boldsymbol{C}_N\} \in \Re^{6N \times 6N}$, where the matrices $\boldsymbol{C}_i \in \Re^{6 \times 6}$ denote the compliance matrix of the grip point i. Next, using the fact that regardless of the force distribution law the spaces $\mathcal{S}_r$ and $\mathcal{S}_a$ are always orthogonal, the total stiffness matrix is given by $\boldsymbol{K}_{tot} = \boldsymbol{N}_a(\boldsymbol{N}_a^{\mathrm{T}} \boldsymbol{C}_0 \boldsymbol{N}_a)^{-1} \boldsymbol{N}_a^{\mathrm{T}}$. The ordinary inverse of $\boldsymbol{K}_{tot}$ does not exist, as this matrix is the $\boldsymbol{C}_0$-orthogonal projection of $\boldsymbol{C}_0^{-1}$ onto the space $\mathcal{S}_a$, and therefore it is singular. However, defining a non-singular transformation between $\Delta \boldsymbol{X}_e$ and $\boldsymbol{F}_a$, we can construct the total compliance matrix in the following form

$$\boldsymbol{C}_{tot} = \boldsymbol{N}_e(\boldsymbol{N}_a^{\mathrm{T}} \boldsymbol{N}_e)^{-1} \boldsymbol{N}_a^{\mathrm{T}} \boldsymbol{C}_0 \boldsymbol{N}_a \boldsymbol{N}_a^{\mathrm{T}}. \quad (6)$$

As can be seen, the constructed compliance matrix is a filter of anergistic forces, with the resulting displacement being always in the space of elastic deformations.

4 Learning Control Loop

In conventional position/force control the compliance parameters of the environment, which in our case is a flexible object handled by the multiple robot arms, are supposed to be known. As has been shown in the previous sections, it is difficult to model the compliance matrices of the real objects precisely. Beside the existing couplings between forces/torques excerted in one direction, and displacements occuring in other directions of the 6-dimensional space, hidden nonlinear effects may appear due to the complex compliance behaviour of the material (physical nonlinearity) or due to the change of configuration (geometrical nonlinearity). In this section we propose a learning control approach, which needs only a rough knowledge of the total compliance matrix $\boldsymbol{C}_{tot}$ as a priori information. The unknown compliance of the object $\boldsymbol{X}_c = \{\boldsymbol{X}_{c_1}^{\mathrm{T}}, \boldsymbol{X}_{c_2}^{\mathrm{T}}, \ldots, \boldsymbol{X}_{c_N}^{\mathrm{T}}\}^{\mathrm{T}} \in \Re^{6N}$, i.e. the combined vector of the spring displacements is learned during the object handling and stored in an associative memory system AMS, a CMAC-based neural network [11, 12]. The AMS is incorporated in the proposed control scheme as an additional feed-forward loop, according to Miller [13] as shown in Figure 4.

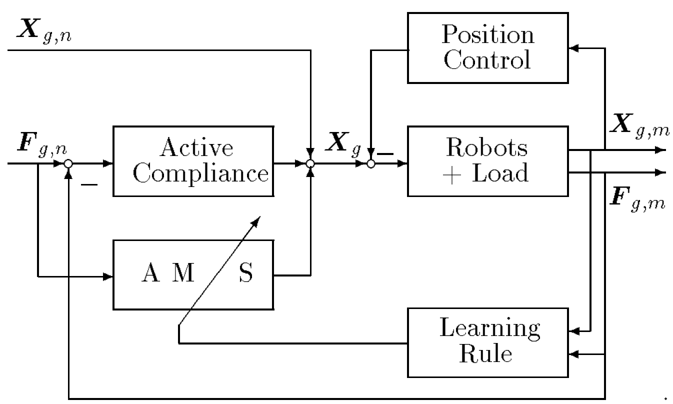

Figure 4: Block-scheme of the learning control system

Although the control scheme is suited for multi-arm robots, for simplicity the learning procedure was formulated and tested only for the case of two arms handling one object. Figure 5 shows the system under consideration where the following transformations are introduced: $\boldsymbol{T}_{R,i}$ are the transformations (expressed as homogenous matrices) to the robot grippers with respect to the reference frame $\mathcal{W}$, $\boldsymbol{T}_{Xc,i}$ are the transformation matrices of the elastic displacements at the grasping points, $\boldsymbol{X}_{c,i}$ the corresponding combined vectors, and $\boldsymbol{T}_{L12} = \boldsymbol{T}(\boldsymbol{\rho}_1)^{-1}\boldsymbol{T}(\boldsymbol{\rho}_2)^{-1}$ is the transformation matrix between the grasping points of the object when not taking the elastic displacements into consideration, where $\boldsymbol{T}(\boldsymbol{\rho}_i)$ represents the transformation corresponding to the vector $\boldsymbol{\rho}_i$.

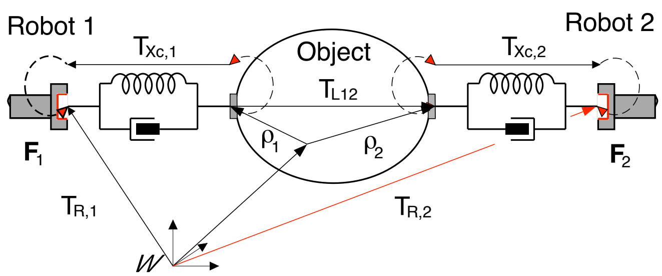

Figure 5: Representation of the virtual object

The goal of the learning procedure is to learn the compliant behaviour of the assumed contact springs i.e. to learn the elastic displacement as function of the applied arm forces $\boldsymbol{X}_{c,i} = f(\boldsymbol{F}_i)$ by observation of the input-output relationship of the system, the commanded position of the robots and the measured arm forces. Since the spring displacements cannot be measured directly they are determined by exploiting the characteristic of the closed kinematic chain. When closing the chain, shown in Figure 5, the following equation has to be met, where $\boldsymbol{I}$ denotes the identity matrix:

$$\boldsymbol{T}_{Xc,1}\boldsymbol{T}_{R,1}^{-1}\boldsymbol{T}_{R,2}\boldsymbol{T}_{Xc,2}^{-1}\boldsymbol{T}_{L12}^{-1} = \boldsymbol{I} \tag{7}$$

As can be seen, the equation above is underdetermined for calculating both spring displacements since only the differences of the positions of the two robots are utilized, i.e the 6-dimensional space of elastic deformation of the object. For that reason, additional constraints are needed. They are obtained by assuming, for simplicity, that the compliance behaviour of both springs is identical. Due to that the trained displacements of both springs can be stored in the same AMS which leads to a better trained memory.

When closing the chain with the assumed or previously learned transformations $\hat{\boldsymbol{T}}_{Xc,i}$ of the elastic displacements we get the following transformation error:

$$\boldsymbol{T}_{Error} = \hat{\boldsymbol{T}}_{Xc,1}\boldsymbol{T}_{R,1}^{-1}\boldsymbol{T}_{R,2}\hat{\boldsymbol{T}}_{Xc,2}^{-1}\boldsymbol{T}_{L12}^{-1} \neq \boldsymbol{I}, \tag{8}$$

which in a rough approximation is $\boldsymbol{T}_{Error} \approx \boldsymbol{T}_{\Delta Xc,1}^{-1} \cdot \boldsymbol{T}_{\Delta Xc,2}$ where $\boldsymbol{T}_{\Delta Xc,i}$ denotes the transformation of the spring displacement with respect to the previously learned displacement $\hat{\boldsymbol{T}}_{Xc,i}$, ($\boldsymbol{T}_{Xc,i} = \hat{\boldsymbol{T}}_{Xc,i} \cdot \boldsymbol{T}_{\Delta Xc,i}$). The corresponding vector errors are denoted by

$$\boldsymbol{X}_{Error} = (x_{ex}, x_{ey}, x_{ez}, x_{e\psi}, x_{e\theta}, x_{e\varphi})^T. \tag{9}$$

The principle of the learning procedure is to modify the vectors of the elastic displacements in each learning step k to reduce this error ($\boldsymbol{X}_{Error} \to \boldsymbol{O}$), by

$$\hat{\boldsymbol{X}}_{c,i}(k) = \hat{\boldsymbol{X}}_{c,i}(k-1) + \beta\boldsymbol{X}_{corr,i}(k), \tag{10}$$

where $\boldsymbol{X}_{corr,i}(k)$ is the correction and β is the learning factor ($0 < \beta \leq 1$). With the assumptions of dominant diagonal elements of the individual compliance matrices and linear behaviour in first approximation, it is possible to distribute the transformation error to corrections of the concentrated springs as follows:

$$\boldsymbol{X}_{corr,i} = \boldsymbol{E} \cdot \boldsymbol{X}_{Error}, \tag{11}$$

$$\text{with: } \boldsymbol{E} = \operatorname{diag}\left[\frac{F_{x,i}}{\sum_{j=1}^{2} F_{x,j}}, \frac{F_{y,i}}{\sum_{j=1}^{2} F_{y,j}}, \frac{F_{z,i}}{\sum_{j=1}^{2} F_{z,j}}, \right. \tag{12}$$

$$\left. \frac{M_{x,i}}{\sum_{j=1}^{2} M_{x,j}}, \frac{M_{y,i}}{\sum_{j=1}^{2} M_{y,j}}, \frac{M_{z,i}}{\sum_{j=1}^{2} M_{z,j}}\right]. \tag{13}$$

5 Simulation results

In this section it is shown that, by use of the introduced learning control loop, the performance of the control system is improved. The learning rule in combination with the Associative Memory (AMS) is capable of learning the load compliance. A transfer motion of the flexible object with applied internal forces has been simulated. To demonstrate the performance of the control loop a trajectory for the internal forces and torques has been determined. The simulated robot positions and forces at the contact points, which can be measured in an experimental setup with wrist force torque sensors, have been used as inputs for the learning rule and the resulting mapping of the spring displacements have been stored as a function of the applied generalized arm forces in the AMS. Due to the assumption of unknown compliance matrices the active compliance controller contains a not adjusted compliance matrix and small gain coefficients to ensure the stability of the control loop. All simulations have been carried out with sampling times of $T_0 = 48ms$ and a delay time of $T_d = 5T_0$ which corresponds to our experimental setup to be used later on. The demonstrated figures depict time histories measured in sampling times on the axis of abscissa.

Figure 6 presents the time history of two simulation runs showing the transformation error on the left side without and on the right side with trained compliances. One component of the simulated and the corresponding learned elastic displacement of both springs are provided in Figure 7.

As can be seen, the applied learning rule is capable to reduce the transformation error by learning the object

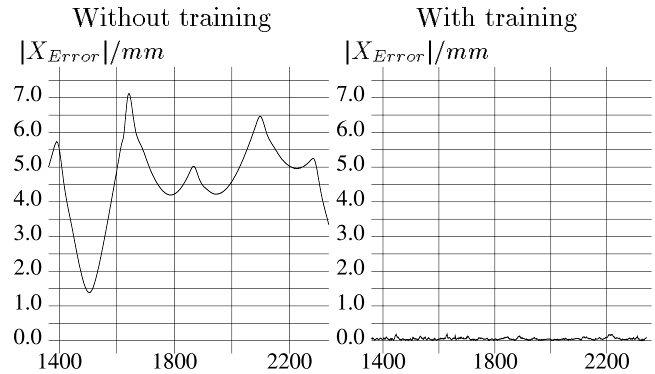

Figure 6: Transformation error according to equation 9

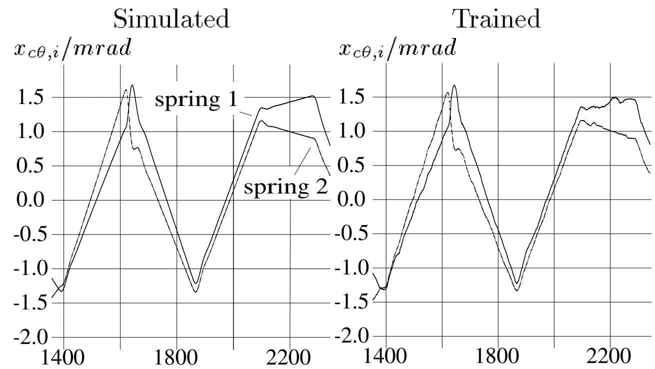

Figure 7: 5th component of the simulated and learned displacement of both springs

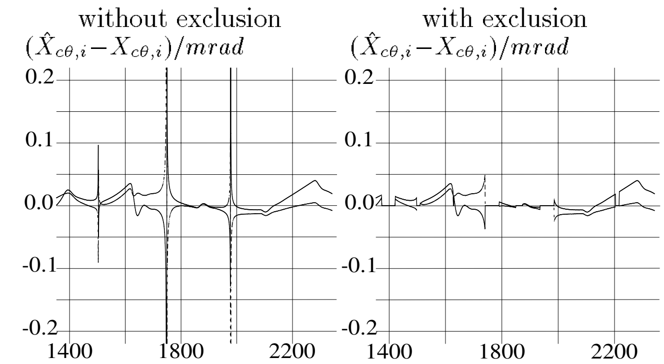

Figure 8: 5th component of the difference between trained and simulated displacement without and with exclusion of singularities in the training rule

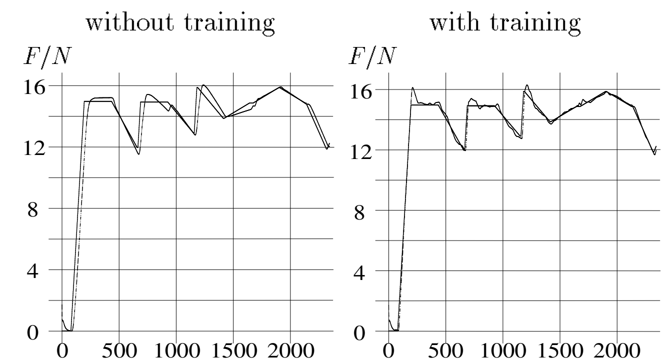

Figure 9: Desired $\boldsymbol{F}_{n,g}$ and actual $\boldsymbol{F}_{m,g}$ displacement of the first component of spring no.1 without training and with training

compliance. By using AMS, a locally generalizing neural net, the learning procedure converges very quickly – the right pictures show the results of the 5th training run.

In the neighbourhood of singularities of the learning rule where one of the denominators in equation 13 becomes 0, ($\sum_{j=1}^{2} F_{i,j} = 0$ or $\sum_{j=1}^{2} M_{i,j} = 0$), the error between trained and simulated displacement $\hat{\boldsymbol{X}}_{c,i}(k) - \boldsymbol{X}_{c,i}(k)$ increases due to measurement errors and coupling terms boosted by the small denominator, which can be seen in the left picture in Figure 8. The resulting peaks which are cutted in the picture reach values till $40mrad$. These areas are excluded from learning by setting the learning factor β to 0. The resulting training error is shown in the picture next to it. This treatment leads to untrained areas in the Associative Memory, which are bridged by the generalizing capabilities of the AMS as can be seen in the previous figure.

The next figures demonstrate the performance of the introduced learning control loop. The system had to follow a desired force/torque trajectory of which the first and most relevant component is presented in Figure 9. Figure 10 shows the resulting Euclidian norm of the force and torque errors respectively, without training, which corresponds to the coordination strategy without the learning control loop presented in Figure 3, and also after the first and the tenth training run.

Without training the elastic deformations necessary for obtaining the desired forces/torques are not calculated by the feedforward terms of the coordination strategy and have to be achieved solely by the not well adjusted controller in the form of a generalized damper, which in previous experiments has turned out to be the best structure for our experimental setup. As can be seen, the controller has problems to follow high gradients of the trajectory (see the corresponding Figure 9). This leads to the high force/torque errors shown in the upper picture of Figure 10. With the learned compliance, i.e. with the static inverse system of the springs the elastic deformations are taken into consideration by the additional feedforward term. The system can follow high gradients of the trajectory better than without this additional loop. Due to the quick convergence of the learning rule there is nearly no further modification after the first training run. Because of the simulated but in the control loop not considered and due to that not learned damping effects, overshoots are generated with changing velocity of the spring displacement. Future investigation has to take this feature into consideration. After training the original feedback controller is used for compensating not modelled effects like damping, measurement noise, and for controlling the system in previously not trained areas.

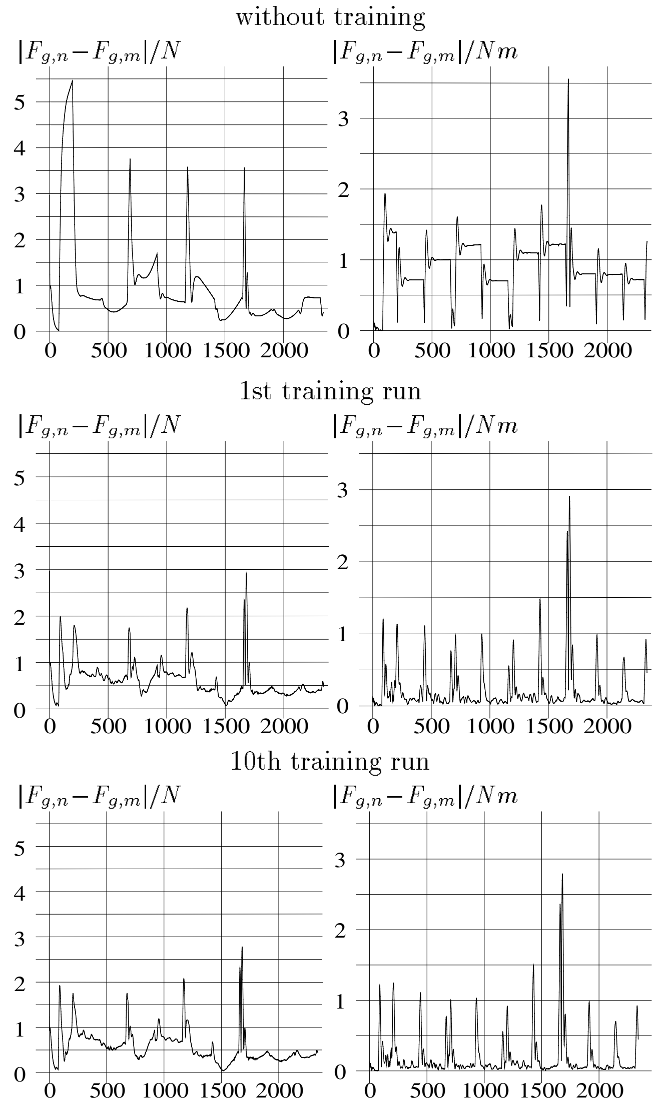

Figure 10: Euclidian norm of the differences between desired and measured forces and torques

6 Conclusions

A task of multi-arm robot control for a transfer motion of flexible objects with changing internal forces has been considered. A mathematical model of the system under consideration has been derived and a control strategy has been formulated. The strategy is based on a decomposition of the position/force parameters in an extended $6N$-dimensional space. The strategy includes feedforward and feedback position/force coordination levels, feedback being constructed in the form of an active compliance control law. An additional feedforward loop has been introduced to take the elastic deformation of the object into consideration. A learning procedure which adapts the unknown compliance behaviour of the object used in the feedforward loop has been presented and tested for the case of two cooperating robots handling one object. The applicability of the learning control loop has been verified by simulation.

Acknowledgements

The study reported in this paper was supported by the Deutsche Forschungsgesellschaft, Graduiertenkolleg "Intelligente Systeme für die Informations- und Automatisierungstechnik" and the Alexander von Humboldt Foundation. We owe special acknowledgement and thanks for the promotion.

References

[1] Cecil O. Alford and Stanley M. Belyeu, "Coordinated Control of two Robot Arms," in *International Conference on Robotics*, 1984.

[2] Y.F. Zheng and J.Y.S Luh, "Control of Two-Arm Coordinated Robots in Motion," in *Proc. 24th IEEE Int. Conf. on Decision and Control*, Fort Lauderdale, 1985, Vol. 3, pp. 1761–1768.

[3] S. Hayati, "Hybrid Position/Force Control of Multi-Arm Cooperating Robot," in *Proc. IEEE Int. Conf. on Robotics and Automation*, San Francisco, 1986, Vol. 1, pp. 82–89.

[4] M. Uchiyama and P. Dauchez, "A Symmetric Hybrid Position/Force Control Scheme for the Coordination of Two Robots," in *Proc. IEEE Int. Conf. on Robotics and Automation*, Philadelphia, 1988, Vol. 1, pp. 350–356.

[5] H. Bruhm and K. Neusser, "An Active Compliance Scheme for Robots with Cooperating Arms," in *Proc. 3rd Int. Conf. on Advanced Robotics*, Versailles, France, 1987, pp. 469–480.

[6] T.J. Tarn, A.K. Bejczy, and X. Yun, "Coordinated Control of Two Robot Arms," in *Proc. IEEE Int. Conf. on Robotics and Automation*, San Francisco, 1986, Vol. 2, pp. 1193–1208.

[7] M.M. Svinin and M. Uchiyama, "Cartesian-level control strategy for a system of manipulators coupled through a flexible object," in *Proc. IEEE/RSJ/GI Int. Conference on Intelligent Robots and Systems, IROS'94*, September 1994, Munich, Germany, Vol. 1, pp. 687–694.

[8] L. Meirovich, *Analytical Methods in Vibrations*, MacMillan Publishing Company, New York, 1967.

[9] M.M. Svinin and Chr. v. Albrichsfeld, "Analysis of Constrained Elastic Manipulations," in *IEEE/RSJ International Conference on Intelligent Robots and Systems*, Pittsburg, USA, 1995.

[10] A. Ben-Israel and T.N.E. Greville, *Generalized Inverses: Theory and Application*, New York, 1974.

[11] J.S. Albus, "A New Approach to Manipulator Control: The Cerebellar Model Articulation Controller (CMAC)," *Transactions of ASME*, 97 (3), 1975.

[12] H. Tolle and E.Ersü, *Neurocontrol: Learning Control Systems Inspired by Neuronal Architectures and Human Problem Solving Strategies*, Berlin, Springer-Verlag, 1992.

[13] W.T. Miller, F.H. Glanz and L.G. Kraft, "Application of a General Learning Algorithm to the Control of Robotic Manipulators," in *The International Journal of Robotics Research*, 1987, Vol. 6 pp. 84-98.